Journal of Medicinal Chemistry

Article

pubs.acs.org/jmc

Inhibition of Galactosyltransferases by a Novel Class of Donor Analogues

Karine Descroix,[†,⊥] Thomas Pesnot,[†,⊥] Yayoi Yoshimura,[‡] Sebastian S. Gehrke,[†,∥] Warren Wakarchuk,[§] Monica M. Palcic,[‡] and Gerd K. Wagner*[,†,∥]

[†]School of Pharmacy, University of East Anglia, Norwich NR4 7TJ, U.K.

[‡]Carlsberg Laboratory, Gamle Carlsberg Vej 10, 1799 Copenhagen V, Denmark

[§]National Research Council Canada, Institute for Biological Science, 100 Sussex Drive, Ottawa, Ontario K1A 0R6, Canada

Supporting Information

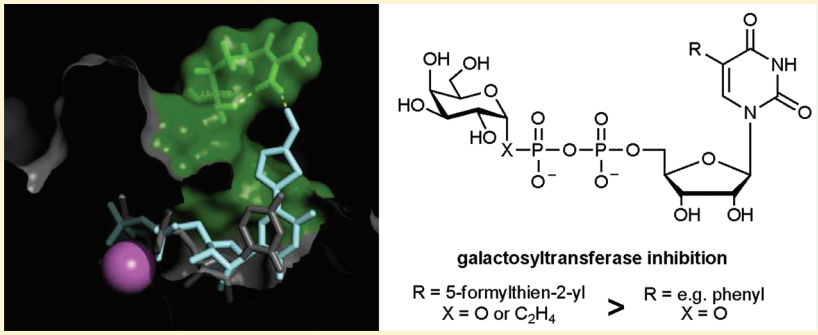

ABSTRACT: Galactosyltransferases (GalT) are important molecular targets in a range of therapeutic areas, including infection, inflammation, and cancer. GalT inhibitors are therefore sought after as potential lead compounds for drug discovery. We have recently discovered a new class of GalT inhibitors with a novel mode of action. In this publication, we describe a series of analogues which provide insights, for the first time, into SAR for this new mode of GalT inhibition. We also report that a new C-glycoside, designed as a chemically stable analogue of the most potent inhibitor in this series, retains inhibitory activity against a panel of GalTs. Initial results from cellular studies suggest that despite their polarity, these sugar-nucleotides are taken up by HL-60 cells. Results from molecular modeling studies with a representative bacterial GalT provide a rationale for the differences in bioactivity observed in this series. These findings may provide a blueprint for the rational development of new GalT inhibitors with improved potency.

INTRODUCTION

Galactosyltransferases (GalTs) are a family of carbohydrate-active enzymes which transfer a D-galactose (D-Gal) residue from the donor UDP-α-D-galactose (UDP-Gal, Figure 1) to a specific acceptor substrate.[1] D-Galactose is an essential component of many biologically and therapeutically important glycan structures, including the human blood group B antigen,[2] the cancer epitopes of the Lewis family (e.g., sialyl Lewis X, sLe^x),[3] and the lipooligosaccharide (LOS) antigen of certain Gram-negative bacteria.[4] GalTs involved in the biosynthesis of these glycan structures have therefore been identified as promising targets for anticancer and anti-infective drug discovery.[5−7] The human galactosyltransferase (GalT) β-1,4-GalT1, for example, catalyzes the galactosylation of GlcNAc- or Glc-based acceptors during sLe^x biosynthesis. Expression levels of β-1,4-GalT1 are elevated in highly metastatic lung cancer,[8] and decoy substrates of β-1,4-GalT1 reduce selectin-mediated tumor metastasis in Lewis lung carcinoma cells.[9] β-1,4-GalT1 therefore represents a promising target for blocking sLe^x formation, and β-1,4-GalT inhibitors are sought after as chemical tools to study these enzymes and processes and as potential anticancer agents.[10−12]

GalTs have also attracted interest as novel targets for antibacterial drug discovery, in particular approaches directed at targeting virulence factors.[13] Gram-negative LOS structures containing a Gal-Gal terminal epitope are important virulence factors for a range of human pathogens including *Neisseria meningitidis* and *Haemophilus influenzae*.[14,15] The terminal oligosaccharides of the bacterial LOS structures mimic human glycolipids and allow the pathogen to evade recognition by the host immune system.[14] A key step in the biosynthesis of LOS structures in some Gram-negative bacteria is the addition of D-Gal onto a terminal lactose, which is catalyzed by the α-1,4-GalT LgtC.[14] The expression of LgtC has been associated with the high-level serum resistance of the nontypeable *Haemophilus influenzae* (NTHI) strain R2866.[15] The primary oligosaccharide glycoform of R2866 contains four heptose and four hexose residues, and the additional D-Gal unit protects the bacterium

Received: August 29, 2011
Published: February 22, 2012

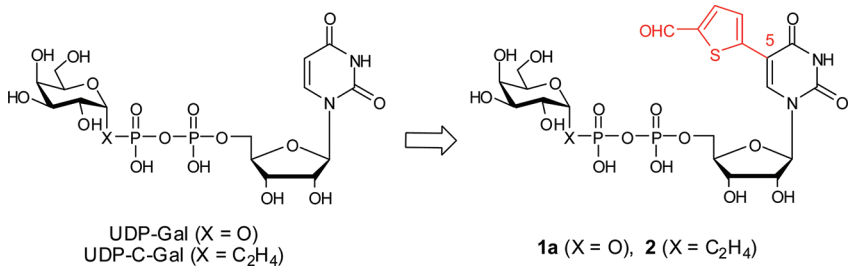

Figure 1. Target design.

Scheme 1. Synthesis of Target Compounds 1a–d and 2[a]

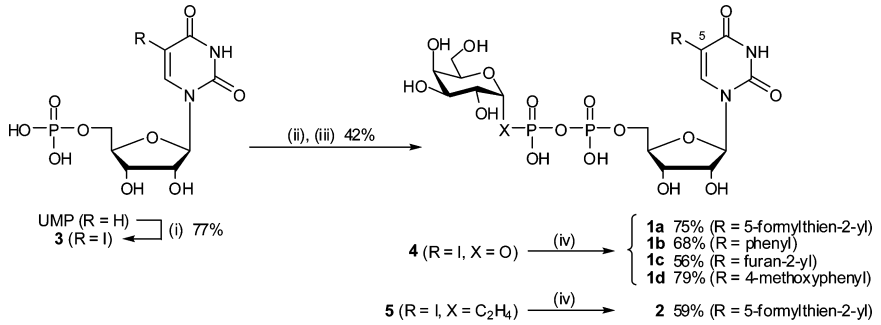

[a]Reagents and conditions: (i) I_2, aq HNO_3, $CHCl_3$, 80 °C, 12 h; (ii) morpholine, 2,2′-dipyridyldisulfide, PPh_3, DMSO, rt, 1 h; (iii) α-D-Gal-1-phosphate, tetrazole, MeCN, DMF, rt, 5 h; (iv) R-B$(OH)_2$, Cs_2CO_3, TPPTS, Na_2Cl_4Pd, H_2O, 50 °C, 20–105 min.

from the human serum response.[15] Inhibition of LgtC has therefore been suggested as a promising strategy for the development of novel antibacterial and antivirulence agents.[14] However, while the crystal structure of *N. meningitidis* LgtC has been solved,[14] no inhibitors for this enzyme have been reported to date.

Despite the considerable potential of GalTs as therapeutic targets, only a limited number of GalT inhibitors have been described to date.[10] Most existing GalT inhibitors are ground-state donor or acceptor analogues whose inhibition constants (K_i) are, at best, of a similar order of magnitude (10–1000 μM) as the K_m value of the respective natural donor or acceptor substrate.[10] We have recently discovered a potent GalT inhibitor with a novel mode of action, which has activity against a range of different GalT enzymes.[16] While previous GalT inhibitors derived from the UDP-Gal donor have usually been modified at the sugar or pyrophosphate moiety, the new inhibitor **1a** is characterized by an additional substituent at the uracil base (Figure 1). Structural and enzymological studies with a representative mammalian blood group GalT suggest that this additional substituent interferes with the folding of an internal loop during the catalytic cycle, which is required for formation of the acceptor binding site, and thus for full catalytic activity.[16] While the cocrystallization structure of this blood group GalT and **1a** raises the possibility that the 5-substituent of **1a** may interact directly with this flexible loop, the flexible loop itself could not be resolved in this structure.[16] At the molecular level, the structural basis for the tight binding and unusual biological activity of the new GalT inhibitor **1a** is therefore presently unclear, as are the ideal structural requirements for the additional substituent in position 5.

In this publication, we explore the scope of this new mode of GalT inhibition. We describe new analogues of the prototypical inhibitor **1a** with different substituents in position 5 and report their biological activity toward different GalTs. These results provide insights, for the first time, into structure–activity relationships (SAR) for this new mode of GalT inhibition. Of particular interest is the activity we observed for these UDP-Gal derivatives against the bacterial enzyme LgtC. Inhibitors of this enzyme have potential as novel antibacterial agents,[14] and the results from this study may provide a template for the rational development of such therapeutics. We also report, for the first time, the GalT-inhibitory activity of a new C-glycosidic analogue of **1a**, UDP-C-Gal **2** (Figure 1), which combines the base-modification of **1a** with a known C-glycosidic motif.[17] We demonstrate that the novel UDP-C-Gal derivative **2** retains the inhibitory activity of its parent sugar-nucleotide **1a** against a panel of GalTs, including LgtC. The improved chemical stability and, potentially, enhanced membrane permeability of this new C-glycoside will facilitate future cellular applications of this novel class of GalT inhibitors.

Target Design. Previously, the development of donor-based GalT inhibitors focused mostly on modifications of the sugar and/or pyrophosphate groups of UDP-Gal,[10] while modifications of the uracil base have not previously been explored. From the analysis of several different GalT structures[14,18,19] we speculated that the donor binding site of these enzymes might be able to accommodate an additional substituent at position 5 of the UDP-Gal donor (Figure S1, Supporting Information). We reasoned that such a modification might be useful for the development of a novel type of GalT inhibitor, and we have recently provided proof-of-principle for this concept with prototype inhibitor **1a**.[16] To explore SAR for this new mode of GalT inhibition, we designed three analogues of **1a** bearing different substituents in position 5. We also sought to exploit the fact that modification of the uracil base, as in **1a**, can be combined with the use of a chemically stable C-glycosidic mimic of the glycosyl linkage, an established strategy for GalT inhibitor design.[17,20,21] These considerations informed the design of the new C-glycoside **2** (Figure 1), which

dx.doi.org/10.1021/jm201154p | J. Med. Chem. 2012, 55, 2015–2024

Table 1. Substrate Activity of Donor Analogues 1a−d and 4 towards Two Different GalTs[a]

		UDP-Gal	1a	1b	1c	1d	4
α-1,3-GalT *B. taurus*	K_m [μM]	118 ± 14	13 ± 1[b]	96 ± 8[b]	69 ± 13[b]	82 ± 11[b]	68 ± 8
	k_{cat} [s^{-1}]	0.98	1.9×10^{-3}	2.1×10^{-3}	4.4×10^{-3}	4.0×10^{-3}	1.6×10^{-3}
β-1,4-GalT *B. taurus*	K_m [μM]	46 ± 8	74 ± 11	274 ± 48	71 ± 11	151 ± 14	nd[c]
	k_{cat} [s^{-1}]	0.65	0.25×10^{-3}	2.2×10^{-3}	1.1×10^{-3}	0.29×10^{-3}	nd[c]

[a]HPLC assay. [b]Reference 30. [c]Not determined.

combines structural features of **1a** and the known GalT inhibitor UDP-C-Gal.[17] We hypothesized that the combination of the base-modification with the C-glycoside motif may not only provide a chemically stable analogue of **1a** but potentially also lead to synergistic inhibitory effects.

RESULTS

Chemical Synthesis. The central step in the synthesis of the target 5-(hetero)aryl UDP-Gal derivatives is the Suzuki−Miyaura coupling of 5-iodo precursors **4** and **5**. This flexible synthetic approach allows the introduction of different 5-substituents in the last step of the synthesis. For the preparation of the new UDP-Gal derivatives **1b−1d**, we adapted the cross-coupling protocol previously developed for the synthesis of 5-(5-formylthien-2-yl) derivatives **1a**[16] and **2**[22] (Scheme 1). Importantly, we managed to improve the synthesis of the cross-coupling substrates **4** and **5**, which starts from 5-iodo UMP **3**. Previously, we had prepared **3** by 5′-selective phosphorylation of 5-iodo uridine.[16] However, the phosphorylation of unprotected nucleosides under Yoshikawa conditions[23] can be complicated by variable yields and the formation of side products. To simplify the preparation of this central intermediate, we adapted previously reported conditions for the iodination of uridine[24] in order to gain access to **3** directly from UMP. Despite the harsh reaction conditions (80 °C, 2 M HNO_3), this approach resulted in the complete iodination of UMP after 12 h and provided 5-iodo UMP **3** in 77% isolated yield after ion-pair purification. Importantly, this approach allowed us to avoid the low-yielding and time-consuming phosphorylation step and provides access to **3** directly from commercially available UMP. Previously, this methodology has only been applied to the iodination of uridine,[24] and this is, to the best of our knowledge, the first example for the direct iodination of UMP. Modified nucleotides have found numerous applications as chemical tools in medicinal chemistry, chemical biology and nanotechnology,[25] and this synthetic method may therefore be of considerable practical interest beyond the present study.

For the preparation of the required cross-coupling substrates **4** and **5**, 5-iodo UMP **3** was converted into the corresponding phosphoromorpholidates under Mukaiyama conditions[26] and coupled with, respectively, galactosyl-1-phosphate and galactosyl-1-ethylphosphonate under tetrazole catalysis (Scheme 1). While 5-iodo UDP-Gal **4** could be prepared relatively efficiently under these conditions within 5 h, with 5-iodo UDP isolated as the only side product in 17% yield, longer reaction times of up to 4 days were required for the formation of the phosphate-phosphonate linkage in **5**.[22] In the final step of the synthesis, the cross-coupling substrates **4** and **5** were reacted successfully with all boronic acids employed in this study to give the target compounds **1a−d** and **2** in 56−79% yield.

Importantly, we found that despite the limited chemical stability of the cross-coupling substrates, the cross-coupling protocol is, in principle, scalable. Thus, the cross-coupling of **4** and **5** with 5-formylthien-2-yl boronic acid was carried out successfully, for the first time, on a 40−50 mg scale. While the cross-coupling of **5** proceeded efficiently on this scale, the isolated yield for **1a** dropped from 75% to 32% under these conditions. In the case of **4**, the reaction time had to be limited to 1.75 h due to the onset of decomposition. Although this is a significantly longer reaction time than for the small-scale reaction (20 min), conversion was incomplete under these conditions. This explains, at least in part, the relatively low isolated yield of **1a**. However, the larger reaction quantities allowed a careful analysis of the side reactions. Unreacted starting material 5-iodo UDP-Gal **4** was isolated in 33%, and several minor decomposition products (5-I UMP, 5-I UDP) were observed by HPLC. Interestingly, the major side product is the parent sugar-nucleotide UDP-Gal, which was isolated in 18% yield. The formation of UDP-Gal resulted from dehalogenation in position 5, a common side reaction under Pd-catalyzed cross-coupling conditions.[27] The same side reaction was also observed during the cross-coupling of **5** with 5-formylthien-2-yl boronic acid, where UDP-C-Gal was isolated as the sole side product in 31% yield. Importantly, this analysis of the competing reactions will allow further optimization of the cross-coupling protocol in the future.

Enzymological Results. The 5-substituted UDP-Gal derivatives were first evaluated as potential donor substrate analogues for the two bovine enzymes α-1,3-GalT and β-1,4-GalT (Table 1). To monitor reaction progress, we established a general HPLC-based assay protocol which allowed us to follow the consumption of UDP-Gal and was applicable with both enzymes. Toward α-1.3-GalT, all 5-(hetero)aryl-substituted UDP-Gal derivatives **1a−d**, as well as 5-iodo UDP-Gal **4**, showed a lower K_m than the natural donor UDP-Gal. The lowest Michaelis−Menten constant in this series was determined for the 5-formylthienyl derivative **1a**, with a 9-fold lower K_m value than UDP-Gal. At the same time, we observed a much slower turnover for all the 5-substituted derivatives than for the natural donor, with k_{cat} values around 3 orders of magnitude lower than for UDP-Gal. Against β-1.4-GalT, it was again the formylthienyl derivative **1a** which showed, together with furan-2-yl derivative **1c**, the lowest K_m of the 5-substituted donor analogues. In this case, all 5-substituted analogues showed a 2−6-fold higher K_m value than the natural donor UDP-Gal but were once again only poor substrates, with 300−2600 fold lower k_{cat} values than UDP-Gal. This enzymological profile, a similar K_m as the natural donor UDP-Gal but a significantly lower k_{cat}, suggested to us that the 5-substituted donor analogues were good to modest binders at these two GalTs, but only relatively poor substrates.

To further investigate this behavior, we analyzed the reaction of α-1.3-GalT with either UDP-Gal or UDP-sugars **1a−c** as potential donors by mass spectrometry. In these experiments, we used lactose linked to a lipid tag at the anomeric position (Lacβ-$O(CH_2)_8CO_2Me$, Figure S2, Supporting Information) as the acceptor to allow the isolation of the galactosylation

dx.doi.org/10.1021/jm201154p | J. Med. Chem. 2012, 55, 2015−2024

Table 2. Inhibitory Activity of UDP-Gal Derivatives 1a–c and 2 against Three Different GalTs[a]

		K_i [μM][b]			
	K_m [μM] UDP-Gal	**1a**	**1b**	**1c**	**2**
GTB	27	2.4 (n = 4)[c]	48	33	3.8
α-1,3-GalT *B. taurus*	77	9.8 (n = 4)[c]	76 (n = 2)	90 (n = 2)	18 (n = 4)
α-1,4-GalT *N. meningitidis*	0.5	0.45[c]	6	1.9	1.7

[a]Radiochemical assay. [b]K_i values were obtained from Dixon plots with the respective inhibitor at three different concentrations (n = 3), unless stated otherwise. [c]Reference 16.

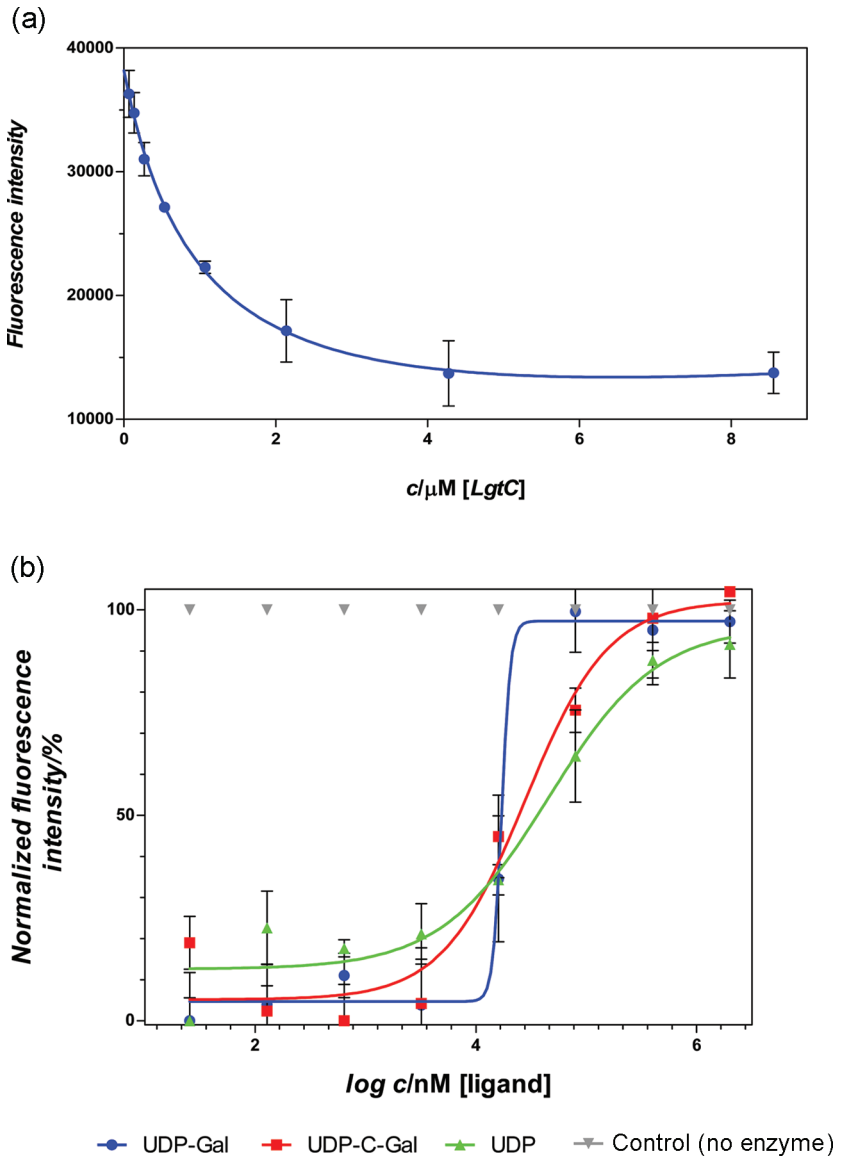

Figure 2. (a) Titration of the fluorescent C-glycoside **2** with α-(1,4)-GalT. Conditions: α-(1,4)-GalT (LgtC from *Neisseria meningitidis*), A/B buffer, 10 min incubation at 37 °C. (b) Competition experiments with α-(1,4)-GalT, fluorophore **2**, and different GalT ligands. Conditions: α-(1,4)-GalT (LgtC from *Neisseria meningitidis*), A/B buffer, 15 min incubation at 37 °C.

product by solid-phase extraction. With the natural donor UDP-Gal, a strong peak of galactosylated acceptor was observed under these conditions, with almost no residual acceptor (Figure S2, Supporting Information). In contrast, with **1a–c** as alternative donors a substantial amount of non-galactosylated acceptor remained even after a prolonged incubation time of 45–80 min, while only a very limited amount of galactosylated acceptor was detected in each case. These results confirmed further, in conjunction with the HPLC data, that although the base-modified UDP-Gal derivatives **1a–c** bind readily to α-1.3-GalT, they are used only very poorly as donor substrates.

This enzymological profile (good binding combined with slow turnover) suggested to us that the 5-substituted UDP-Gal derivatives may be able to act as inhibitors of galactosylation. We therefore studied the inhibitory activity of derivatives **1a–c** toward three different GalTs in a radiochemical assay,[18] coincubating each donor analogues with the respective enzyme

dx.doi.org/10.1021/jm201154p | *J. Med. Chem.* 2012, 55, 2015–2024

and acceptor as well as radiolabeled UDP-Gal. Under these conditions, all 5-substituted UDP-Gal derivatives inhibited the transfer of radiolabeled galactose to acceptor, albeit with variable potency (Table 2). The formylthienyl-substituted derivative **1a** was the most potent inhibitor against all three enzymes, with K_i values in the range of, or below, the K_m for the natural donor substrate UDP-Gal. The 5-phenyl (**1b**) and 5-furan-2-yl (**1c**) substituted derivatives showed weaker activity. These differences in potency between **1a** and **1b**/**1c** were enzyme-dependent: they were greatest against the human blood group enzyme GTB (14−20-fold) and less pronounced against the bacterial α-1.4-GalT LgtC (4−13-fold).

C-Glycoside **2**. Although our initial enzymological experiments showed that 5-substituted UDP-Gal derivatives are only very poor donor substrates for GalTs, it can be argued that their residual donor substrate activity, although very modest, may complicate their application as chemical tools in cellular studies. To eliminate any residual donor substrate activity, we designed a nonhydrolyzable congener of UDP-Gal derivative **1a** in which the glycosidic linkage is replaced with a C-glycosidic isostere. We also speculated that such a modification my lead to additional benefits such as improved cell penetration and enhanced inhibitory potency. The design of this new C-glycoside **2** was informed by the combination of the 5-substituent in **1a** with UDP-C-Gal, a known GalT inhibitor.[17] The inhibitory activity of C-glycoside **2** was assessed in the radiochemical assay against three different GalTs (Table 2). Pleasingly, compound **2** showed effective inhibition against all GalTs tested although with slightly weaker potency than the parent UDP-sugar **1a**. The strongest inhibition was observed against the bacterial α-1.4-GalT LgtC. The K_i values against GTB and α-1.3-GalT, while 1.6−1.8-fold higher than those of **1a** against the same enzymes, are still significantly lower than the K_m (UDP-Gal) for these GalTs.

Next, we decided to investigate the binding specificity of the new UDP-C-Gal derivative **2**. We and others have shown that 5-substituted uridine nucleotides and sugar-nucleotides with a suitable substituent in position 5 are strongly fluorescent.[28−30] We have previously demonstrated that due to this autofluorescence, 5-substituted UDP-Gal derivatives such as **1a** can be used as fluorescent sensors for GalTs, as their fluorescence is quenched upon specific binding at the target enzyme.[30] UDP-C-glycoside **2** possesses similar fluorescence characteristics as its parent UDP-Gal derivative **1a**, which allowed us to carry out a range of fluorescence-based binding experiments. LgtC was selected as the GalT of choice for these experiments, as **2** showed the lowest K_i value against this enzyme.

In titration experiments with LgtC, the fluorescence of **2** was quenched by the enzyme in a concentration-dependent manner (Figure 2a). This observation is in agreement with results previously obtained for the parent UDP-sugar **1a** in similar experiments[30] and indicates that **2** is a good binder at LgtC. To investigate the specificity of the binding, we next carried out ligand-displacement experiments. Importantly, the fluorescence-quenching effect for **2**/LgtC can be reversed by increasing concentrations of unlabeled UDP-Gal and UDP, two specific ligands at the donor binding site of LgtC (Figure 2b). These results therefore suggest that C-glycoside **2** binds specifically at the donor binding site of LgtC and that its fluorescence quenching is not simply due to nonspecific binding at the protein surface. Results from these displacement experiments can also be used to calculate IC_{50} values for the known LgtC ligands UDP and UDP-Gal (UDP-Gal 17 μM; UDP 46 μM). **2** may therefore also be useful as a chemically stable fluorophore for GalT screening assays, as previously described for **1a**.[30] Interestingly, UDP-C-Gal also effectively displaces **2** from LgtC (IC_{50} 28 μM), providing the first experimental evidence that this type of C-glycoside binds at the donor binding site of a GalT.

Cellular Uptake Studies. We also exploited the strong fluorescence of **1a** and **2** to study their cellular uptake by fluorescence microscopy, in order to assess if the new inhibitors might be suitable for cellular applications. Upon incubation of HL-60 cells for 24 h with stock solutions of **1a** and **2**, the blue fluorescence emission (λ_{em} 434 nm characteristic for the 5-(5-formylthien-2-yl) uracil fluorophore was visible intracellularly in intact, viable cells (Figure S3, Supporting Information). This result suggests that despite their polarity, these inhibitors are taken up into mammalian cells, possibly through passive diffusion or endocytosis. **1a** appears to localize preferentially to the ER and Golgi, as would be expected from a sugar-nucleotide, while the distribution of **2** appears to be more diffuse.

DISCUSSION AND MOLECULAR MODELING

From the enzymological studies, a trend emerges for the effect of the 5-substituent on GalT inhibition. Generally, the two donor analogues bearing a 5-formylthien-2-yl substituent (**1a** and **2**) were the most potent GalT inhibitors, while other substituents in position 5 were less effective. GTs frequently undergo significant conformational rearrangement of the active site during catalysis. In the case of GalTs, the movement of one or more flexible loops over the UDP-Gal donor assists in the formation of the acceptor binding site.[31] We have previously shown that **1a** inhibits a mammalian blood group GalT by blocking this flexible loop movement during the catalytic cycle.[16] The close structural and mechanistic similarities within the GalT family[31] suggested that this novel mode of inhibition might also be applicable to LgtC and other GalTs. Importantly, the new results in the present manuscript support this idea. On the basis of the previous results, we hypothesized that the blocking of the flexible loop may be due simply to a steric interaction with the 5-substituent.[16] However, the new results in the present manuscript suggest that steric bulk alone in position 5 is not sufficient for this mode of GalT inhibition. Rather, the weaker activity of analogues **1b** and **1c** suggests that the 5-formylthienyl substituent in **1a** and **2** may interact specifically with a particular residue in the flexible loop of the target enzyme.

To investigate this possibility, and to understand the basis for the superiority of the 5-formylthienyl substituent in inhibiting GalT activity, we carried out molecular docking studies with UDP-Gal derivatives **1a**−**c** and UDP-C-Gal **2**. For these studies, we focused on the bacterial α-1.4-GalT LgtC, as the 5-substituted UDP-Gal derivatives showed the lowest K_i values against this particular enzyme. In addition, LgtC inhibitors would be useful templates for the development of novel antibacterial agents. In the case of LgtC, two small loops fold over the donor during catalysis,[14] and this loop movement may be blocked by an additional, sterically demanding substituent in position 5 of the UDP-Gal donor. However, the differences in activity observed within our series of donor analogues suggest that steric factors alone do not account for LgtC inhibitory activity via this mechanism.

All base-modified UDP-Gal derivatives, including the C-glycoside **2**, could be docked into the donor binding site of

dx.doi.org/10.1021/jm201154p | J. Med. Chem. 2012, 55, 2015−2024

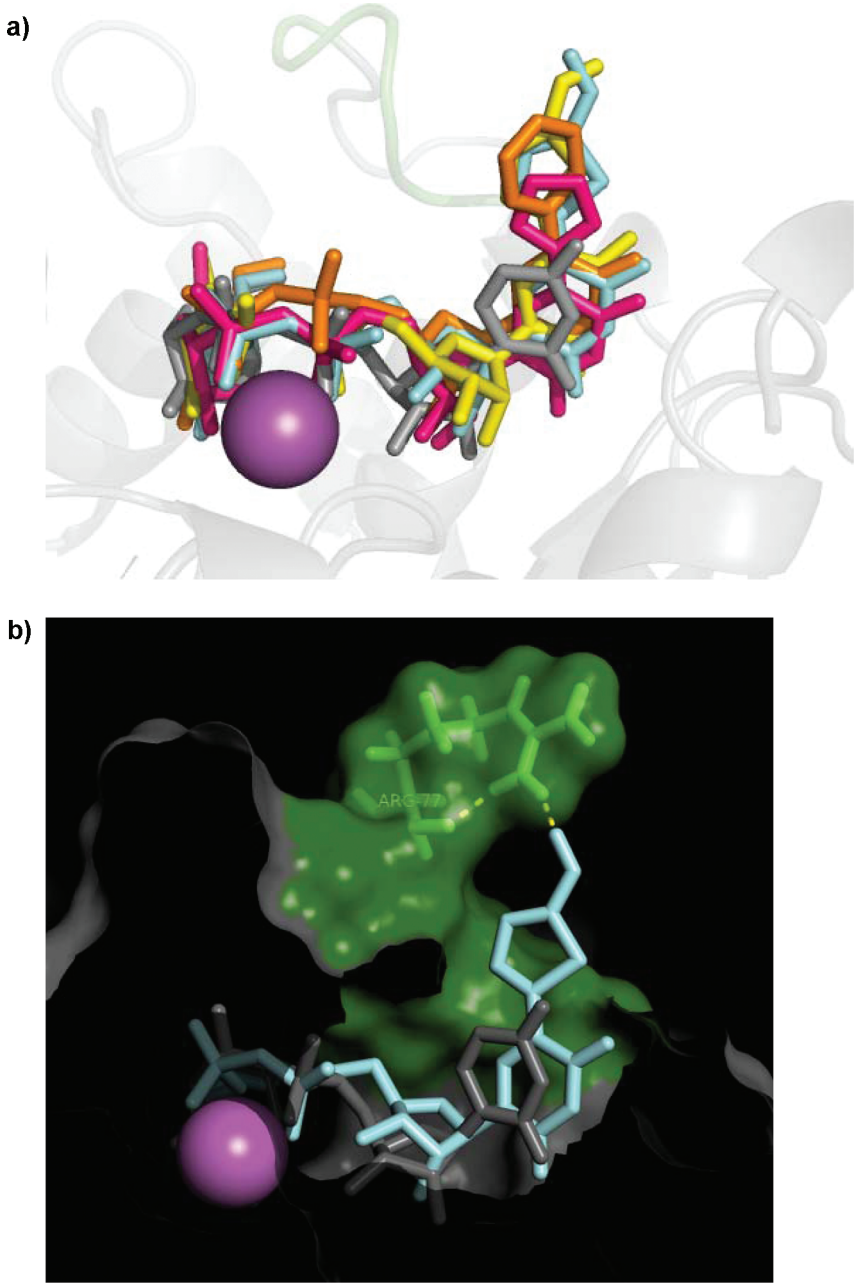

Figure 3. (a) Overlay of docking solutions for **1a** (cyan), **1b** (orange), **1c** (magenta), and **2** (yellow) with the cocrystallized ligand UDP-2F-Gal (gray) in the donor binding site of LgtC. Mn^{2+} is shown in purple, and residues 75−80 in the flexible loop of the protein are shown in green. (b) Surface representation of the donor binding site of LgtC, with the docking solution for **1a** (cyan) and the original ligand UDP-2F-Gal (gray) shown in sticks. The hydrogen bond between the formyl group of **1a** and Arg77 is represented as a yellow dotted line. Residues 75−80 in the flexible loop of the protein are shown in green, including Arg77, which is shown in sticks. Mn^{2+} is shown in purple. Residues Asp10 and Tyr11 have been omitted for clarity.

LgtC in a similar orientation as the natural donor UDP-Gal (Figure 3). The poses of the docked ligands replicate important interactions observed in the cocrystal with the original ligand UDP-2F-Gal, including the coordination of the pyrophosphate linkage with a manganese ion in the active site and a $\pi-\pi$ stacking interaction between the uracil ring and Tyr11. The donor binding site in LgtC is buried to a large extent inside the protein, with only the upper face of the uracil base accessible by solvent.[14] Our docking results suggest that the additional substituent in position 5 of UDP-Gal derivatives **1a**−**c** and **2** is accommodated into this cleft, pointing toward one of the flexible loops of LgtC (Figure 3a). In this orientation, the 5-substituent is well positioned not only to sterically interfere with the folding of the loop over the uracil base but also to potentially form specific interactions with individual loop residues. Interestingly, the highest ranked docking solutions for **1a** and its C-glycosidic analogue **2** consistently show a hydrogen bond between the formyl group of these two donor analogues and the guanine of Arg77, a possible interaction that is unique to **1a** and **2** (Figure 3b). The specific interaction with Arg77 may therefore offer an explanation for the superior potency of the 5-formylthien-2-yl substituted derivatives. While an exclusively steric interaction of donor analogue and loop, as in the case of **1b** and **1c**, may be sufficient to block loop folding,

dx.doi.org/10.1021/jm201154p | J. Med. Chem. 2012, 55, 2015−2024

the additional hydrogen bond with Arg77 may provide additional stabilization for the ligand/enzyme complex, resulting in the stronger inhibition observed for **1a** and **2**.

As a similar trend of **1a** and **2** being better inhibitors than **1c** and **1d** was also observed for bovine α-1.3-GalT and the blood group GalT GTB, we also analyzed available crystal structures of these two enzymes. Structural alignments of the three proteins suggest that Arg194 in α-1.3-GalT[32] and Arg100 in GTB[18] occupy a similar position in the flexible loop of the two mammalian enzymes as Arg77 in LgtC (Figure S4, Supporting Information). This suggests that upon binding of ligand, these Arg residues may adopt a similar orientation relative to the 5-position of the donor or donor analogue as Arg77 in LgtC. The presence of this conserved Arg residue and its potential interaction with the 5-formylthienyl substituent in **1a** and **2** may therefore provide a structural basis for the similar bioactivities that were observed in this series against all three enzymes.

CONCLUSION

Herein, we describe the first series of structural analogues for a new class of GalT inhibitors. This series includes a new C-glycoside which is similarly potent as the parent UDP-Gal derivative. We show that a new mode of GalT inhibition, which we have recently discovered,[16] is broadly applicable within this enzyme class. In addition, the biological results with different GalTs provide, for the first time, insights into SAR for this mode of inhibition: our results suggest that the 5-formylthienyl substituent in our prototype inhibitor **1a** cannot simply be replaced by another sterically demanding substituent. Rather, in addition to steric bulk, a specific interaction with the flexible loop of the target GalT may be important for this mode of action. In the case of LgtC, our molecular modeling experiments suggest that this specific interaction may come from hydrogen bonding of the 5-formylthienyl substituent with Arg77. In principle, this interaction could be exploited for the development of inhibitors with enhanced potency, as well as for the design of GalT-selective inhibitors. Our molecular docking results provide a blueprint for the rational design of such second-generation inhibitors. The development of such inhibitors will be greatly facilitated by the improved synthetic route described herein, and knowledge of the side reactions will facilitate the preparation of new 5-substituted UDP-Gal derivatives for further biological studies in this exciting new inhibitor class.

EXPERIMENTAL SECTION

General. All reagents were obtained commercially and used as received unless stated otherwise. UDP-C-Gal[17], 5-iodo UDP-C-Gal **5**[22] and α-D-galactose-1-phosphate[33] were prepared as previously reported. Anhydrous solvents sold on molecular sieves were used as such. Anhydrous acetonitrile was obtained by distillation over CaH_2 under nitrogen atmosphere. All moisture sensitive reactions were carried out under an atmosphere of nitrogen in oven-dried glassware. TLCs were performed on precoated aluminum plates (Silica Gel 60 F_{254}, Merck), with IPA:H_2O:NH_3 (6:3:1) as the mobile phase unless otherwise stated. Compounds were visualized by exposure to UV light (254/280 nm) and/or by staining with anisaldehyde reagent. The identity and purity of all products was determined by ^1H, ^{13}C, and ^{31}P NMR spectroscopy, high-resolution mass spectrometry (HRMS), and HPLC. All test compounds met the required purity criteria (>95% by HPLC). NMR spectra were recorded at 298 K on a Varian VXR 400 S spectrometer (400 MHz for ^1H, 100 MHz for ^{13}C, 161.9 MHz for ^{31}P). Chemical shifts (δ) are reported in ppm and referenced to methanol (δ_H 3.34, δ_C 49.50 for solutions in D_2O). Coupling constants (J) are reported in Hz. Proton-signal assignments were made by first-order analysis of the spectra as well as analysis of 2D $^1H-^1H$ correlation maps (COSY). The ^{13}C NMR assignments are supported by 2D $^{13}C-^1H$ correlations maps (HSQC). Accurate electrospray ionization mass spectra (HR ESI-MS) were obtained on a Finnigan MAT 900 XLT mass spectrometer at the EPSRC National Mass Spectrometry Service Centre, Swansea. Analytical HPLC was carried out on a PerkinElmer Series 200 machine equipped with a Supelcosil LC-18-T column (5 μm, 25 cm × 4.6 mm), a column oven (set to 35 °C), and a diode array detector. Compound purity was analyzed under the following conditions: buffer A, potassium phosphate (100 mM), tetrabutylammonium bisulfate hydrogen sulfate (8 mM), pH 6.5; buffer B, buffer A/methanol (70/30), pH 6.5. Elution gradient: 0–50% buffer B over 15 min, 50% buffer B for 1.5 min, 50–0% buffer B over 1.5 min, and 100% buffer A for 7 min. Preparative chromatography was performed on a Biologic LP chromatography system equipped with a peristaltic pump and a 254 nm UV optics module under the following conditions:

Ion-Pair Chromatography. Ion-pair chromatography was performed using Lichroprep RP-18 resin equilibrated with 0.05 M TEAB. Gradient: MeOH or MeCN against 0.05 M TEAB over a total volume of 480 mL. Flow rate: 5 mL/min. Product-containing fractions were combined and reduced to dryness. The residue was coevaporated repeatedly with methanol to remove residual TEAB.

Anion Exchange Chromatography. Anion exchange chromatography was performed using MacroPrep 25Q resin, either in a glass column or a pre-packed MacroPrep High Q cartridge (5 mL). Gradient: 0–100% 1 M TEAB (pH 7.3) against H_2O over a total volume of 480 mL. Flow rate: 5 mL/min (glass column) or 2–3 mL/min (cartridge). Product-containing fractions were combined and reduced to dryness. The residue was coevaporated repeatedly with methanol to remove residual TEAB.

General Method for the Preparation of 5-(Hetero)aryl UDP-α-D-galactose Derivatives 1a–d. A 2-necked round-bottom flask with **4** (1 equiv), Cs_2CO_3 (2–2.5 equiv), and the requisite (hetero)arylboronic acid (1.5 equiv) was purged with N_2. TPPTS (0.0625 equiv), Na_2Cl_4Pd (0.025 equiv), and degassed H_2O (4 mL) were added, and the reaction was stirred under N_2 for the required time at 50 °C. Upon completion, the reaction was cooled to room temperature and the pH was adjusted to 7 with 1% HCl. The suspension was filtered through a membrane filter (0.45 μm). The filter was washed with H_2O, and the combined filtrates were evaporated under reduced pressure. The residue was purified by anion-exchange chromatography and/or ion-pair chromatography. Product-containing fractions were combined and reduced to dryness, and the residue was coevaporated repeatedly with methanol to remove excess TEAB.

5-(5-Formylthien-2-yl) UDP-α-D-galactose (1a). The title compound was prepared from **4** (8.6 mg, 12.4 μmol) and 5-formylthien-2-ylboronic acid according to the general method (reaction time: 20 min). After purification by ion-pair chromatography (gradient: 0–20% MeCN), the triethylammonium salt of **1a** was obtained as a glassy solid in 75% yield (7.9 mg). HPLC: 10.10 min (96%). ^1H NMR (400 MHz, D_2O) δ_H 3.66–3.72 (2H, m, H-6″), 3.72–3.76 (1H, m, H-2″), 3.84 (1H, dd, J = 3.2 and 10.3 Hz, H-3″), 3.95 (1H, d, J = 3.3 Hz, H-4″), 4.10–4.13 (1H, m, H-5″), 4.28–4.31 (2H, m, H-5′), 4.32–4.34 (1H, m, H-4′), 4.40–4.48 (2H, 2t, J = 5.2 and 9.4 Hz, H-2′, H-3′), 5.62 (1H, dd, J = 3.5 and 7.2 Hz, H-1″), 6.03 (1H, d, J = 4.8 Hz, H-1′), 7.72 (1H, d, J = 4.2 Hz, H-thienyl), 8.00 (1H, d, J = 4.2 Hz, H-thienyl), 8.44 (1H, s, H-6), 9.79 (1H, s, CHO). ^{13}C NMR (125.8 MHz, D_2O) δ_C 61.7, 65.7 (d, J = 4.6 Hz), 69.0 (d, J = 6.7 Hz), 69.7, 70.0, 70.3, 72.6, 74.9, 84.3 (d, J = 7.3 Hz), 89.7, 96.4 (d, J = 5.4 Hz), 109.6, 126.0, 139.2, 140.3, 142.0, 144.8, 151.2, 163.5, 187.8. ^{31}P NMR (121.5 MHz, D_2O) δ_P −11.2 (d, J = 22.5 Hz), −12.7 (d, J = 21.2 Hz). m/z (ESI) 675.0305 $[M - H]^-$, $C_{20}H_{25}N_2O_{18}P_2S$ requires 675.0304.

5-Phenyl UDP-α-D-galactose (1b). The title compound was prepared from **4** (16 mg, 23 μmol) and phenylboronic acid according to the general method (reaction time: 30 min). After sequential

dx.doi.org/10.1021/jm201154p | J. Med. Chem. 2012, 55, 2015–2024

purification by ion-pair (gradient: 0−20% MeCN) and ion exchange chromatography, the triethylammonium salt of **1b** was obtained as a glassy solid in 68% yield (11.6 mg). HPLC: 9.94 min (95%). ^{1}H NMR (400 MHz, D_2O) δ_H 1.27 (2.0 equiv of TEA, t, J = 6.8 Hz), 3.19 (2.0 equiv of TEA, q, J = 6,8 Hz), 3.64−3.72 (2H, m, H-6″), 3.75 (1H, dt, J = 2.8 and 8.4 Hz, H-2″), 3.87 (1H, dd, J = 3.2 and 10.3 Hz, H-3″), 3.98 (1H, d, J = 3.2 Hz, H-4″), 4.13 (1H, t, J = 6.2 Hz, H-5″), 4.17−4.21 (2H, m, H-5′), 4.28−4.32 (1H, m, H-4′), 4.39 (1H, t, J = 4.6 Hz, H-3′), 4.48 (1H, t, J = 5.5 Hz, H-2′), 5.59 (1H, dd, J = 3.5 and 7.2 Hz, H-1″), 6.04 (1H, d, J = 6.0 Hz, H-1′), 7.40−7.56 (5H, m, Ph), 7.88 (1H, s, H-6). ^{13}C (125 MHz, D_2O) δ_C 9.0 (TEA), 47.5 (TEA), 61.7 (C-6″), 65.9 (C-5′), 69.0 (d, $J_{C,P}$ = 7.9 Hz, C-2″), 69.7 (C-4″), 69.9 (C-3″), 70.6 (C-3′), 72.6 (C-5″), 74.1 (C-2′), 84.1 (d, $J_{C,P}$ = 9.4 Hz, C-4′), 89.1 (C-1′), 96.5 (d, $J_{C,P}$ = 6.0 Hz, C-1″), 117.0 (C-5), 129.0 (*i*Ph), 129.3, 129.4 (*o*Ph, *m*Ph), 132.3 (*p*Ph), 139.1 (C-6), 152.2 (C-2), 165.6 (C-4). ^{31}P NMR (121 MHz, D_2O) δ_P −11.4 (d, $J_{P,P}$ = 20.6 Hz,), −12.8 (d, $J_{P,P}$ = 20.6 Hz). m/z (ESI) 660.1199 $[M + NH_4]^+$, $C_{21}H_{32}N_3O_{17}P_2$ requires 660.1201.

5-(2-Furyl)-UDP-α-D-galactose (1c). The title compound was prepared from **4** (7.2 mg, 10.4 μmol) and furan-2-ylboronic acid according to the general method (reaction time: 30 min). After purification by ion-pair chromatography (gradient: 0−10% MeCN), the triethylammonium salt of **1c** was obtained as a glassy solid in 56% yield (4.9 mg). HPLC: 9.18 min (95%). ^{1}H NMR (400 MHz, D_2O) δ_H 1.27 (1.4 equiv of TEA, t, J = 6.8 Hz), 3.19 (1.4 equiv of TEA, q, J = 6,8 Hz), 3.64−3.74 (2H, m, H-6″), 3.77 (1H, dt, J = 3.4 and 8.4 Hz, H-2″), 3.88 (1H, dd, J = 3.3 and 10.3 Hz, H-3″), 3.97 (1H, d, J = 3.2 Hz, H-4″), 4.14 (1H, dd, J = 4.6 and 7.6 Hz, H-5″), 4.22−4.27 (2H, m, H-5′), 4.30−4.34 (1H, m, H-4′), 4.43 (1H, t, J = 4.6 Hz, H-3′), 4.49 (1H, t, J = 5.4 Hz, H-2′), 5.63 (1H, q, J = 3.6 Hz, H-1″), 6.06 (1H, d, J = 5.6 Hz, H1′), 6.53 (1H, dd, J = 1.8 and 3.4 Hz, fur3), 6.90 (1H, d, J = 3.4 Hz, fur4), 7.59 (1H, d, J = 1.8 Hz, fur2), 8.24 (1H, s, H-6). ^{13}C (125 MHz, D_2O) δ_C 9.0 (TEA), 47.5 (TEA), 61.8 (C-6″), 66.0 (d, $J_{C,P}$ = 5.0 Hz, C-5′), 69.1 (d, $J_{C,P}$ = 8.2 Hz, C-2″), 69.8 (C-3″), 70.0 (C-4″), 70.6 (C-3′), 72.7 (C-5″), 74.3 (C-2′), 84.2 (d, $J_{C,P}$ = 10.1 Hz, C-4′), 89.2 (C-1′), 96.6 (d, $J_{C,P}$ = 5.6 Hz, C-1″), 108.4 (C-5), 109.6 (fur4), 112.2 (fur3), 136.2 (C-6), 143.4 (fur2), 146.0 (fur1), 151.7 (C-2), 163.4 (C-4). ^{31}P NMR (121 MHz, D_2O) δ_P −11.4, −12.7. m/z (ESI) 650.0990 $[M + NH_4]^+$, $C_{19}H_{30}N_3O_{18}P_2$ requires 650.0994.

5-(4-Methoxyphenyl)-UDP-α-D-galactose (1d). The title compound was prepared from **4** (9.7 mg, 14 μmol) and 4-methoxyphenylboronic acid according to the general method (reaction time: 25 min). After sequential purification by ion-pair (gradient: 0−20% MeCN) and ion exchange chromatography, the triethylammonium salt of **1d** was obtained as a glassy solid in 79% yield (9.7 mg). HPLC: 11.43 min (98%). ^{1}H NMR (400 MHz, D_2O) δ_H 1.27 (2.1 equiv of TEA, t, J = 6.8 Hz), 3.19 (2.1 equiv of TEA, q, J = 6,8 Hz), 3.64−3.70 (2H, m, H-6″), 3.75 (1H, dt, J = 3.0 and 11.0 Hz, H-2″), 3.86 (1H, dd, J = 3.5 and 10.0 Hz, H-3″), 3.87 (3H, s, MeO), 3.97 (1H, d, J = 3.2 Hz, H-4″), 4.12 (1H, dd, J = 4.6 and 7.6 Hz, H-5″), 4.17−4.21 (2H, m, H-5′), 4.28−4.32 (1H, m, H-4′), 4.39 (1H, dd, J = 3.5 and 5.0 Hz, H-3′), 4.47 (1H, t, J = 5.7 Hz, H-2′), 5.59 (1H, dd, J = 3.6 and 7.0 Hz, H-1″), 6.04 (1H, d, J = 6.0 Hz, H-1′), 7.07, 7.49 (4H, 2d, J = 8.9 and 8.9 Hz, *o*Ph, *m*Ph), 7.84 (1H, s, H-6). ^{13}C (125 MHz, D_2O) δ_C 9.0 (TEA), 47.5 (TEA), 56.0 (MeO), 61.8 (C-6″), 66.1 (d, $J_{C,P}$ = 6.8 Hz, C-5′), 69.1 (d, $J_{C,P}$ = 7.8 Hz, C-2″), 69.2 (C-3″), 70.0 (C-4″), 70.7 (C-3′), 72.7 (C-5″), 74.1 (C-2′), 84.3 (d, J = 10.1 Hz, C-4′), 89.1 (C-1′), 96.6 (d, $J_{C,P}$ = 7.0 Hz, C-1″), 114.9 (*m*Ph), 116.7 (C-5), 125.1 (*i*Ph), 130.9 (*o*Ph), 138.5 (C-6), 152.4 (C-2), 159.6 (*p*Ph), 165.8 (C-4). ^{31}P NMR (121.5 MHz, D_2O) δ_P −11.3 (d, $J_{P,P}$ = 20.6 Hz), −12.8 (d, $J_{P,P}$ = 20.6 Hz). m/z (ESI) 690.1314 $[M + NH_4]^+$, $C_{22}H_{34}N_3O_{18}P_2$ requires 690.1307.

5-(5-Formylthien-2-yl) UDP-C-galactose (2). A 2-necked round-bottom flask with **5** (ref 22,56.7 mg, 0.070 mmol), 5-formylthien-2-ylboronic acid (20.0 mg, 0.127 mmol, 1.8 equiv), and Cs_2CO_3 (39 mg, 0.162 mmol, 2.3 equiv) in degassed H_2O (5 mL) was purged with N_2. TPPTS (2.5 mg, 0.004 mmol, 0.06 equiv) and Na_2Cl_4Pd (0.5 mg, 0.002 mmol, 0.03 equiv) were added to the mixture, and the reaction was stirred under N_2 for 1.75 h at 55 °C. The reaction mixture was cooled to room temperature and purified by ion-pair chromatography to give the triethylammonium salt of the title compound as a glassy solid in 59% yield (38 mg). HPLC: 11.28 min (99%). ^{1}H NMR (400 MHz, D_2O) δ_H 9.76 (s, 1H, C*H*O), 8.44 (s, 1H, H6), 7.98 (d, 1H, J = 4.2 Hz, $H_{thiophene}$), 7.73 (d, 1H, J = 4.2 Hz, $H_{thiophene}$), 6.01 (d, 1H, $J_{1'-2'}$ = 4.8 Hz, H1′), 4.44 (t, 1H, $J_{2'-3'}$ = 4.8 Hz, H2′), 4.41 (t, 1H, $J_{3'-4'}$ = 4.8 Hz, H3′), 4.33−4.28 (m, 1H, H4′), 4.28−4.22 (m, 2H, H5′a, H5′b), 3.95−3.89 (m, 2H, H3″, H4″), 3.85 (dd, 1H, $J_{6'',7''}$ < 1 Hz, H6″), 3.71 (dd, 1H, $J_{5'',6''}$ = 3.4 Hz, $J_{4'',5''}$ = 9.4 Hz, H5″), 3.67−3.55 (m, 3H, H7″, H8″a, H8″b), 3.16 (q, J = 7.3 Hz, CH_2 TEA, 2.2 equiv), 1.93−1.52 (m, 4H, H1″a, H1″b, H2″a, H2″b), 1.23 (t, 20.3H, CH_3 TEA, 2.2 equiv). ^{13}C (150.9 MHz, D_2O) δ_C 187.1 (*C*HO), 163.5 (C4), 151.2 (C2), 144.5 (C6), 141.3, 139.6, 138.3, 125.2, 108.9 (5C, C5, 4$C_{thiophene}$), 89.1 (C1′), 83.5 (d, $J_{C,P}$ = 8.9 Hz, C4′), 75.6 (d, $J_{C,P}$ = 18.2 Hz, C3″), 74.2 (C2′), 71.4 (C7″), 69.5, 69.5, 69.0 (3C, C3′, C5″, C6″), 68.3 (C4″), 64.7 (C5′), 61.1 (C8″), 23.8 (d, $J_{C,P}$ = 140.0 Hz, C1″), 18.2 (d, $J_{C,P}$ < 5 Hz, C2″). ^{31}P NMR (161.9 MHz, D_2O) δ_P 20.1 (d, $J_{P,P}$ = 27.2 Hz, C*P*OPO), −10.4 (d, $J_{P,P}$ = 27.2 Hz, CPO*P*O). m/z (ESI) 687.0651 $[M - H]^-$, $C_{22}H_{29}N_2O_{17}P_2S_1$ requires 687.0668.

Enzymology. *N. meningitidis* α-(1,4)-GalT, *B. taurus* α-(1,3)-GalT, and *Homo sapiens* GTB were expressed and purified as previously reported.[14,34] The β-(1,4)-GalT from bovine milk was purchased from Sigma (G5507). HPLC-based enzyme assays with α-(1,3)-GalT and β-(1,4)-GalT were carried out as previously described.[16] A/B buffer contained MOPS (50 mM, pH 7.0), $MnCl_2$ (20 mM), and bovine serum albumin (1 mg/mL) and was prepared by 1:10 dilution of a 10× A/B buffer stock solution (500 mM MOPS, 200 mM $MnCl_2$, 10 mg/mL BSA). The radiochemical enzyme assays were carried out according to the previously reported protocol.[18,35] In brief, the following procedure was observed (described for compound **2** as a representative example, comparable conditions were used for **1a−c**): the reaction was started by adding GalT solution (5 μL) to each substrate mixture (10 μL; donor + acceptor + various concentrations of compound **2**). The reaction mixture (total volume 15 μL) was incubated for 15 min at 37 °C. The reaction was stopped by adding water (500 μL). K_i values were determined by Dixon plot analysis ($1/v$ vs inhibitor concentration) using GraphPad Prism. Each GalT was assayed in the following incubation mixture (all concentrations are final concentrations). *N. meningitidis* α-(1,4)-GalT (prior to addition to the reaction mixture, the enzyme was activated with DTT[14]): UDP-Gal (0.57 μM), 83000 dpm of UDP-(^{3}H)-Gal, Lacβ-O$(CH_2)_8CO_2$Me (2 mM), compound **2** (0, 3.125, 6.25, and 12.5 μM) DTT 1.7 mM, and α-(1,4)-GalT (diluted 1:27000 from stock, 0.010 ng) in A/B buffer (pH 7); Dixon plot: r^2 = 0.984. *H. sapiens* GTB: UDP-Gal (26 μM), 101000 dpm of UDP-(^{3}H)-Gal, Fucα1,2Galβ-O$(CH_2)_7CH_3$ (500 μM), compound **2** (0, 31.25, 46.875, and 62.5 μM), and GTB (diluted 1:3300 from stock, 0.049 ng) in A/B buffer (pH 7); Dixon plot: r^2 = 0.978. *B. taurus* α-(1,3)-GalT: UDP-Gal (76 μM), 102000 dpm of UDP-(^{3}H)-Gal, Lacβ-O$(CH_2)_8CO_2$Me (500 μM), compound **2** (0, 15.625, 31.25, 46.875, and 62.5 μM), and α-(1,3)-GalT (diluted 1:670, 1.3 μg) in A/B buffer (pH 7); Dixon plot: r^2 = 0.999.

Mass Spectrometry Experiments. UDP-Gal or donor analogues **1a−c** (8 mM, 4 mL), Lacβ-O$(CH_2)_8CO_2$Me (10 mM, 2 mL), A/B buffer (2 mL), H_2O (2 mL), and *B. taurus* α-(1,3)-GalT (10 mL, ca. 200 mU/mL) were incubated at rt for the given time (UDP-Gal, 70 min; **1a**, 78 min; **1b**, 45 min; **1c**, 55 min). The reaction was stopped by addition of H_2O (600 mL), and the samples were filtered through a Sep-Pak column. The column was washed with H_2O (4×), and then eluted with methanol (1 mL). The methanol eluate was analyzed on a Bruker Esquire 3000 Plus mass spectrometer in ESI mode.

Fluorescence Experiments. Fluorescence intensity measurements were carried out in black NUNC F96 MicroWell polystyrene plates on a BMG labtech PolarStar microplate reader equipped with a 350 ± 5 nm excitation filter and a 430 ± 5 nm emission filter. Titration experiment: Samples were added to individual microplate wells as follows (total volume/well: 200 μL; all concentrations are final concentrations/well); A/B buffer (40 μL), water (80 μL), fluorophore **2** (200 nM, 40 μL), *N. meningitidis* α-(1,4)-GalT (40 μL, dilutions of protein stock **E1−E8**: 1/5, 1/10, 1/20, 1/40, 1/80, 1/160, 1/320, 1/640). The fluorescence emission was measured after 10 min at 37 °C

dx.doi.org/10.1021/jm201154p | J. Med. Chem. 2012, 55, 2015−2024

and plotted against LgtC dilutions with GraphPad Prism 5. All experiments were carried out in triplicate. Fluorophore displacement experiments: Samples were added to the requisite microplate wells as follows (total volume/well: 200 μL; all concentrations are final concentrations/well); A/B buffer (80 μL), fluorophore **2** (200 nM, 40 μL), *N. meningitidis* α-(1,4)-GalT (40 μL, 1/100 dilution of protein stock). The samples were incubated for 20 min at 37 °C. After this time, unlabeled ligand (UDP-Gal, UDP, or UDP-C-Gal) was added to the requisite well (40 μL, concentrations **L1**−**L8**: 25.6 nM, 128 nM, 640 nM, 3.2 μM, 16 μM, 80 μM, 400 μM, 2 mM). The samples were incubated for 15 min at 37 °C, and the fluorescence emission was measured. For each ligand concentration, control experiments with A/B buffer (40 μL) instead of enzyme were carried out by following the same protocol. All experiments were carried out in triplicate. For the calculation of IC_{50} values, data points were fitted to a 4-parameter curve with GraphPad Prism 5. Prior to this step, the raw data were normalized as follows: the maximum fluorescence F_L^{max} (i.e., control experiments for each ligand **L**) and the minimum fluorescence F_L^{min} (i.e., fluorescence at a ligand **L** concentration of 25.6 nM) were normalized to, respectively, 100% and 0% for each set of experiments. For each ligand concentration, the measured fluorescence intensity was then converted to a percentage of the maximum fluorescence according to the following equation: $F_{\%} = (F_L - F_L^{min}) \times 100/(F_L^{max} - F_L^{min})$.

Cellular Uptake Studies. HL-60 cells (LGC Promochem, Middlesex, UK) were grown in RPMI 1640 medium supplemented with 16.7% (v/v) heat-inactivated fetal calf serum, L-glutamine (2 mL, 200 mM), and PenStrep (1 mL, 5000 units). Cells were seeded in a final concentration of 10^6 cells/mL and incubated at 37 °C and 5% CO_2 for 24 h in the presence of a glass coverslip and donor analogues **1a** or **2** (100 μM) in their sodium salt form. After 24 h, the coverslip was washed with medium to remove extracellular fluorophore and to minimize background fluorescence. The immobilized cells were analyzed by confocal fluorescence microscopy. Images were recorded on an Axioplan2 Imaging Zeiss microscope equipped with the picture processing software Axioplan (wavelengths: 364 nm/1.0%, 488 nm/0.1%). The intracellular location of the blue fluorescence indicated cellular uptake of **1a** and **2**.

Molecular Modeling. All calculations were performed on an Intel Core Duo 2.8Ghz MacBook Pro. The crystal structure of galactosyltransferase LgtC in complex with donor and acceptor sugar analogues was obtained from the RCSB Protein Data Bank (PDB code 2G8A). The protein was prepared for molecular modeling analysis using the MOE modeling package (CCG, Montreal, Canada). The ligand UDP-2F-Gal and crystallographic water molecules were removed, leaving an empty active center with the acceptor sugar still in place. Hydrogen atoms were added to the heavy atoms, and the residues were assigned with the appropriate protonation states at pH 7.4. The final protein was saved in TriposMol2 format. The molecule was directly imported into the GOLD software package (CCDC, Cambridge, UK, Version 3.2) for subsequent docking calculations. The UDP-Gal analogues **1a**−**c** and **2** were built with the Builder module of MOE, and hydrogen atoms were assigned to all heavy atoms in the molecules. All ligands were energy minimized using the MMFF94s force field and the conjugate gradient method, until the default derivative convergence criterion of 0.01 kcal/mol × A was met. The individual phosphate and phosphonate groups were assigned a charge of −1, as appropriate at pH 7.4. The ligand files were exported into GOLD as Tripos Mol2 files. The docking of the substrates into the catalytic site of 1GA8 was carried out using Gold Suite 4.12 (CCDC, Cambridge, UK). The binding site was defined by the position of UDP-2F-Gal in the original structure and the radius was set to 15 Å. The residues Asp8, Asn10, Tyr11, Arg77, His78, Ile79, Ser80, Ile81, Thr82, and Thr83 were defined as flexible using the rotamer library option.[36] All torsion angles in each inhibitor were allowed to rotate freely. GoldScore was chosen as the scoring function, and the solutions were rescored using the ChemScore scoring function. The GA settings were adjusted to a search efficiency of 200%. For each ligand, 200 docking runs were performed. The resulting solutions were clustered on the basis of heavy atom rmsd values (1 Å). The top-ranked solutions were visually analyzed using MOE and MacPymol (PyMOL Molecular Graphics System, Version 1.3, Schrödinger, LLC). To validate the docking protocol, the inhibitor UDP-2F-Gal was redocked into the empty catalytic pocket of LgtC using the above protocol, and the conformations of the top scored poses were compared to the crystal structure position of the ligand. All docking poses were exported as sdf files and imported into MOE as a database (mdb file). The script fragment_superpose.svl (CCG) was used to calculate the rmsd values. In the default settings the option for "ignore chirality" was unticked. The rmsd value for the redocked ligand was 0.52.

■ ASSOCIATED CONTENT

Supporting Information

Figures, experimental procedures and spectroscopic data for compounds **3** and **4**, and NMR spectra of compounds **1a**−**d**, **2** and **4**. This material is available free of charge via the Internet at http://pubs.acs.org.

■ AUTHOR INFORMATION

Corresponding Author

*Phone: +44 (0)20 7848 4747. Fax: +44 (0)20 7848 4045. E-mail: gerd.wagner@kcl.ac.uk.

Present Address

[‖]Institute of Pharmaceutical Science, School of Biomedical Sciences, King's College London, Waterloo Campus, Franklin-Wilkins Building, 150 Stamford Street, London, SE1 9NH, U.K.

Author Contributions

[⊥]Equal contribution

Notes

The authors declare no competing financial interest.

■ ACKNOWLEDGMENTS

We thank the EPSRC (First Grant EP/D059186/1, to G.K.W.), the MRC (Discipline Hopping Award G0701861, to G.K.W.), the Royal Society (Research Grant, to G.K.W.), and the Danish Natural Science Research Council FNU (to M.M.P.) for financial support. We thank Dr Dietmar Steverding (UEA) and Dr Paul Thomas (UEA) for assistance with the cellular uptake studies and the fluorescence microscopy work. We are grateful to Durita Djurhuus for excellent technical assistance and to the EPSRC National Mass Spectrometry Service Centre, Swansea, for the recording of mass spectra.

■ REFERENCES

(1) Hennet, T. The galactosyltransferase family. *Cell. Mol. Life Sci.* **2002**, *59*, 1081−1095.

(2) Patenaude, S. I.; Seto, N. O. L.; Borisova, S. N.; Szpacenko, A.; Marcus, S. L.; Palcic, M. M.; Evans, S. V. The structural basis for specificity in human ABO(H) blood group biosynthesis. *Nature Struct. Biol.* **2002**, *9*, 685−690.

(3) Pudelko, M.; Bull, J.; Kunz, H. Chemical and chemoenzymatic synthesis of glycopeptide selectin ligands containing Sialyl Lewis X structures. *ChemBioChem* **2010**, *11*, 904−930.

(4) Zhu, P.; Boykins, R. A.; Tsai, C.-M. Genetic and functional analyses of the lgtH gene, a member of the β-1,4-galactosyltransferase gene family in the genus Neisseria. *Microbiology* **2006**, *152*, 123−134.

(5) Schutzbach, J.; Brockhausen, I. Inhibition of glycosyltransferase activities as the basis for drug development. In *Methods in Molecular Biology Vol. 534. Glycomics: Methods and Protocols*; Packer, N. H., Karlsson, N. G., Eds.; Humana Press, Totowa, NJ, 2009; pp359−373.

(6) Brown, J. R.; Crawford, B. E.; Esko, J. D. Glycan antagonists and inhibitors: a fount for drug discovery. *Crit. Rev. Biochem. Mol. Biol.* **2007**, *42*, 481−515.

(7) Dube, D. H.; Bertozzi, C. R. Glycans in cancer and inflammation: potential for therapeutics and diagnostics. *Nature Rev. Drug. Discovery* **2005**, *4*, 477−488.
(8) Zhu, X. Y.; Jiang, J. H.; Shen, H. L.; Wang, H. Z.; Zong, H. L.; Li, Z. J.; Yang, Y. Z.; Niu, Z. Y.; Liu, W. C.; Chen, X. N.; Hu, Y.; Gu, J. X. Elevated β-1,4-galactosyltransferase I in highly metastatic human lung cancer cells. *J. Biol. Chem.* **2005**, *280*, 12503−12516.
(9) Brown, J. R.; Yang, F.; Sinha, A.; Ramakrishnan, B.; Tor, Y.; Qasba, P. K.; Esko, J. D. Deoxygenated disaccharide analogs as specific inhibitors of β-1−4-galactosyltransferase 1 and selectin-mediated tumor metastasis. *J. Biol. Chem.* **2009**, *284*, 4952−4959.
(10) For recent reviews on GT inhibitors see: (a) Qian, X.; Palcic, M. M. Glycosyltransferase inhibitors. In *Carbohydrates in Chemistry & Biology*; Ernst, B., Hart, G., Sinaÿ, P., Eds.; Wiley-VCH: Weinheim, 2000; pp 293−328; (b) Kajimoto, T.; Node, M. Synthesis of glycosyltransferase inhibitors. *Synthesis* **2009**, 3179−3210. (c) Roychoudhury, R.; Pohl, N. L. B. New structures, chemical functions, and inhibitors for glycosyltransferases. *Curr. Opin. Chem. Biol.* **2010**, *14*, 168−173.
(11) Takaya, K.; Nagahori, N.; Kurogochi, M.; Furuike, T.; Miura, N.; Monde, K.; Lee, Y. C.; Nishimura, S.-I. Rational design, synthesis, and characterization of novel inhibitors for human β-1,4-galactosyltransferase. *J. Med. Chem.* **2005**, *48*, 6054−6065.
(12) Hosoguchi, K.; Maeda, T.; Furukawa, J.-I.; Shinohara, Y.; Hinou, H.; Sekiguchi, M.; Togame, H.; Takemoto, H.; Kondo, H.; Nishimura, S.-I. An efficient approach to the discovery of potent inhibitors against glycosyltransferases. *J. Med. Chem.* **2010**, *53*, 5607−5619.
(13) Escaich, S. Antivirulence as a new antibacterial approach for chemotherapy. *Curr. Opin. Chem. Biol.* **2008**, *12*, 400−408.
(14) Persson, K.; Ly, H. D.; Dieckelmann, M.; Wakarchuk, W. W.; Withers, S. G.; Strynadka, N. C. J. Crystal structure of the retaining galactosyltransferase LgtC from *Neisseria meningitidis* in complex with donor and acceptor sugar analogs. *Nature Struct. Biol.* **2001**, *8*, 166−175.
(15) Erwin, A. L.; Allen, S.; Ho, D. K.; Bonthius, P. J.; Jarisch, J.; Nelson, K. L.; Tsao, D. L.; Unrath, W. C. T.; Watson, M. E.; Gibson, B. W.; Apicella, M. A.; Smith, A. L. Role of l*gtC* in resistance of nontypeable *Haemophilus influenzae* strain R2866 to human serum. *Infect. Immun.* **2006**, *74*, 6226−6235.
(16) Pesnot, T.; Jørgensen, R.; Palcic, M. M.; Wagner, G. K. Structural and mechanistic basis for a new mode of glycosyltransferase inhibition. *Nature Chem. Biol.* **2010**, *6*, 321−323.
(17) Vidal, S.; Bruyere, I.; Malleron, A.; Auge, C.; Praly, J.-P. Non-isosteric C-glycosyl analogues of natural nucleotide diphosphate sugars as glycosyltransferase inhibitors. *Bioorg. Med. Chem.* **2006**, *14*, 7293−7301.
(18) Alfaro, J. A.; Zheng, R. B.; Persson, M.; Letts, J. A.; Polakowski, R.; Bai, Y.; Borisova, S. N.; Seto, N. O. L.; Lowary, T. L.; Palcic, M. M.; Evans, S. V. ABO(H) blood group A and B glycosyltransferases recognize substrate via specific conformational changes. *J. Biol. Chem.* **2008**, *283*, 10097−10108.
(19) Gastinel, L. N.; Cambillau, C.; Bourne, Y. Crystal structures of the bovine beta-4-galactosyltransferase catalytic domain and its complex with uridine diphosphogalactose. *EMBO J.* **1999**, *18*, 3546−3557.
(20) Waldscheck, B.; Streiff, M.; Notz, W.; Kinzy, W.; Schmidt, R. R. α-(1−3)-Galactosyltransferase inhibition based on a new type of disubstrate analogue. *Angew. Chem., Int. Ed.* **2001**, *40*, 4007−4011.
(21) Schäfer, A.; Thiem, J. Synthesis of novel donor mimetics of UDP-Gal, UDP-GlcNAc, and UDP-GalNAc as potential transferase inhibitors. *J. Org. Chem.* **2000**, *65*, 24−29.
(22) Descroix, K.; Wagner, G. K. The first C-glycosidic analogue of a novel galactosyltransferase inhibitor. *Org. Biomol. Chem.* **2011**, *9*, 1855−1862.
(23) Yoshikawa, M.; Kato, T.; Takenishi, T. A novel method for phosphorylation of nucleosides to 5′-nucleotides. *Tetrahedron Lett.* **1967**, *50*, 5065−5068.
(24) Flasche, W.; Cismas, C.; Herrmann, A.; Liebscher, J. Lipophilic nucleosides by Sonogashira coupling. *Synthesis* **2004**, *14*, 2335−2341.
(25) Cobb, A. J. A. Recent highlights in modified oligonucleotide chemistry. *Org. Biomol. Chem.* **2007**, *5*, 3260−3275.
(26) Mukaiyama, T.; Hashimoto, M. Phosphorylation by oxidation-reduction condensation. Preparation of active phosphorylating reagents. *Bull. Chem. Soc. Jpn.* **1971**, *44*, 2284.
(27) Fairlamb, I. J. S. Regioselective (site-selective) functionalisation of unsaturated halogenated nitrogen, oxygen and sulfur heterocycles by Pd-catalysed cross-couplings and direct arylation processes. *Chem. Soc. Rev.* **2007**, *36*, 1036−1045.
(28) Sinkeldam, R. W.; Greco, N. J.; Tor, Y. Fluorescent analogs of biomolecular building blocks: design, properties, and applications. *Chem. Rev.* **2010**, *110*, 2579−2619.
(29) Pesnot, T.; Wagner, G. K. Novel derivatives of UDP-glucose: Concise synthesis and fluorescent properties. *Org. Biomol. Chem.* **2008**, *6*, 2884−2891.
(30) Pesnot, T.; Palcic, M. M.; Wagner, G. K. A novel fluorescent probe for retaining galactosyltransferases. *ChemBioChem* **2010**, *11*, 1392−1398.
(31) Qasba, P. K.; Ramakrishnan, B.; Boeggeman, E. Substrate-induced conformational changes in glycosyltransferases. *Trends Biochem. Sci.* **2005**, *30*, 53−62.
(32) Jamaluddin, H.; Tumbale, P.; Withers, S. G.; Acharya, K. R.; Brew, K. Conformational changes induced by binding UDP-2F-galactose to alpha-1,3 galactosyltransferase- implications for catalysis. *J. Mol. Biol.* **2007**, *369*, 1270−1281.
(33) Posternak, T. Synthesis of α-D-glucose-1-phosphate and α-D-galactose-1-phosphate. *J. Am. Chem. Soc.* **1950**, *72*, 4824−4825.
(34) Sujino, K.; Uchiyama, T.; Hindsgaul, O; Seto, N. O. L.; Wakarchuk, W. W.; Palcic, M. M. Enzymatic synthesis of oligosaccharide analogues: evaluation of UDP-Gal analogues as donors for three retaining α-galactosyltransferases. *J. Am. Chem. Soc.* **2000**, *122*, 1261−1269.
(35) Palcic, M. M.; Heerze, L. D.; Pierce, M.; Hindsgaul, O. The use of hydrophobic synthetic glycosides as acceptors in glycosyltransferase assays. *Glycoconjugate J.* **1988**, *5*, 49−63.
(36) Lovell, S. C.; Word, J. M.; Richardson, J. S.; Richardson, D. C. The penultimate rotamer library. *Proteins* **2000**, *40*, 389−408.